

# New Vistas in Weak Lensing

## 1 Overview and Objectives

Weak gravitational lensing has emerged as one of the powerful probes of cosmology. The small distortions of background images as they are lensed by foreground matter are sensitive to both the contents and the geometry of the Universe (e.g., Blandford and Narayan (1992), Hoekstra and Jain (2008)). Galaxy images are the most commonly used cosmological sources (see Kilbinger (2015) and references therein), but weak lensing of the cosmic microwave background (CMB) is also widely studied (see e.g., the review by Lewis and Challinor (2006), and results from, e.g., the Planck satellite, Ade *et al.* 2015). These two implementations of lensing differ not only in the sources studied but also in the fundamental observable. In one case, the shapes of galaxies are used to determine the intervening gravitational potential (see the top left panel in Figure 1, which shows galaxy clusters and large-scale structure). On the other hand, for the CMB, the potential can be mapped (middle panel of Figure 1) using *anisotropies* in the two-point statistics of the otherwise Gaussian field.

These *anisotropic two-point functions* (hereafter ATF) will affect any cosmologically distributed background sources. The field of weak lensing can therefore be broadened by looking at new applications of them. We choose three to work on in this proposal:

(1) **The Ly $\alpha$  forest**- as the angular positions of quasars are deflected, the forest in quasar spectra is also lensed. In Croft et al. (2018) (hereafter C18) the PI proposed measurement of the ATF of the Ly $\alpha$  forest.

(2) **The ATF of the angular galaxy distribution** relies on the same physics. The positions of galaxies are deflected by lensing resulting in local distortions of clustering statistics.

(3) **A new window on time delays with ATF**. So far, time delays have been detected only in the case of strong lensing. But using our new technique, upcoming CMB experiments can estimate the time delay field.

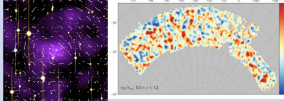
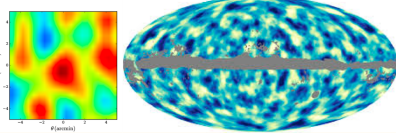
| Effect\Source                               | Galaxies  | Cosmic Microwave Background  | Lyman alpha Forest |
|---|---|--|--------------------|
| Ellipticities due to deflection             |  | Not Applicable   | Not Applicable     |
| Anisotropic 2-pt function due to deflection | This Proposal   |  | This Proposal      |
| Anisotropic 2-pt function due to Time Delay |   | This Proposal  |                    |

Figure 1: New vistas: anisotropies of the 2-pt. function in galaxy clustering, CMB time delay, and the Ly $\alpha$  forest

We will carry out an in depth study of these three new weak lensing applications of ATF spanning theory and simulations, from first detections to precision cosmology. We will study them together in order to benefit from their common aspects, and common simulations. Our specific objectives are as follows:

(a) **to simulate new lensing tracers**, the forest, galaxy clustering and time delay anisotropy, including non-linear physics, baryonic effects and observational systematic errors.

(b) **to develop statistical techniques** for the analysis of new lensing data, including cross-correlations and mass reconstruction, and use knowledge from our full simulations to address and mitigate systematics.

(c) **to make observational measurements** from first detections to competitive determinations of  $\sigma_8$  at the 3% level from forest and galaxy datasets, the CLAMATO, eBOSS and DES surveys.

(d) **to explore new cosmological constraints** from these measurements which have different strengths and potential biases to other lensing results.

## 2 Anisotropic two point functions

The successful implementations of lensing so far (galaxy shear and CMB ATF ) are similar in that they both are sensitive to – and therefore can be used to measure – the projected gravitational potential as a function of position on the sky:

$$\Phi(\vec{\theta}) = \frac{2}{c^2} \int_0^{D(z_s)} \frac{dD}{D(z_s)} \frac{D(z_s, z)}{D} \phi(\vec{x}), \quad (1)$$

where  $\phi$  is the 3D potential at the position  $\vec{x} = \vec{x}[\vec{\theta}, D(z)] \rightarrow [D(z)\vec{\theta}, D(z)]$  in the small angle limit;  $D(z)$  is the angular diameter distance to redshift  $z$  and  $D(z, z')$  is the angular diameter distance between redshifts  $z$  and  $z'$ .

Since so much of this proposal will be based on the anisotropy in the 2-point statistics and because this idea is relatively new (Hu, 2001) compared with the easier to understand shape measurements, it is worth spending a paragraph explaining the basic idea. Since the universe is homogeneous and anisotropic, the two-point function of any observable, e.g., the temperature on the surface of last scattering:  $C(\phi) = \langle T(\vec{\theta})T(\vec{\theta} + \vec{\phi}) \rangle$  depends only on the magnitude of  $\phi$ . When expanded in terms of spherical harmonics with coefficients  $a_{lm}$ , this property leads directly to the relation

$$\langle a_{lm} a_{l'm'}^* \rangle = \delta_{ll'} \delta_{mm'} C_l. \quad (2)$$

When photons from one part of the sky travel through an over-dense region and from another through an under-dense region, the situation changes and now the 2-point function depends not only on angular distance between two points but also on the position on the sky. The product of  $a_{lm}$  and  $a_{l'm'}$  now will have non-zero expectation even when  $l \neq l'$ , an expectation value that is proportional to the field that breaks the isotropy,  $\Phi$ . By forming quadratic estimators with  $lm$  and  $l'm'$  slightly different, we can obtain an estimate for the potential (Hu, 2001; Hu and Okamoto, 2002). This effect is what we call anisotropic two-point functions, ATF.

ATF of the CMB field has proved fruitful, but it is not the only possibility, as any light emitted at cosmological distances is deflected on its way to us and therefore the statistics of any set of sources will be anisotropic. With the huge growth in surveys of the Universe we now have the exciting possibility of expanding the way gravitational lensing is done and treating new fields and new observations as sources. In the context of this more general view of weak lensing, we have chosen three of the most promising to focus on, the Lyman-alpha forest, angular galaxy clustering, and CMB time delay anisotropies. Fig. 1 gives a schematic view of the new vistas that open up as a result.

In principle, time delays can also impact the two-point functions of galaxies (Fig. 1, left, bottom) and the Lyman alpha forest (Fig. 1, right, bottom), but we think the current focus of the proposal on the three shaded boxes in Fig. 1 presents a broad range of opportunities for students: ranging from guaranteed detections that could become competitive to more speculative ideas that will likely yield detections. In these latter cases, more work is needed to demonstrate that they can provide information competitive with the more traditional lensing methods.

A final introductory comment related to the pair of pictures in the upper left and middle panels of Fig. 1: The impact of lensing is easiest to detect in *cross-correlation*. The left-most picture in each of those panels depicts a detection of lensing due to galaxy clusters, in one case by measuring the tangential shear of background galaxies and in the other by measuring the ATF of the CMB behind clusters. The noise in the auto-correlation is larger, so in each case, the first detection came in the cross-correlation regime (with clusters as the lenses). We expect something similar in our cases, although throughout this proposal we will weave back and forth between the signal due to clusters and that due to large scale structure in general. Ultimately, we expect both types of signals to be detectable in all of our three probes.

### 2.1 Ly $\alpha$ forest lensing

For the first probe, the Ly $\alpha$  forest, the ATF will be measured from the large-scale structure of the intergalactic medium, as seen in quasar spectra. The forest has the advantage of spectral information, potentially yielding

many lensed “slices” at different redshifts. An idealized test was carried out in C18 using a mock high resolution angular grid of quasars (of order arcminute separation) and a linear theory foreground density field. Standard quadratic estimators (e.g., Hu and Okamoto (2002)) were used to successfully reconstruct images of the foreground mass distribution. In the work proposed here we will expand the realism of such tests and make measurements on real data. Enough work has been done to date on this source that this is a relatively low risk project. There is still the question of how powerful a tool ATF of the Ly $\alpha$  forest statistics will become. Will they surpass the more traditional shape measurements for at least some range of redshift? What are the systematics that must be treated in order to extract cosmological information? We argue below that we are well-suited to address these questions and feel that they provide a broad range of opportunities for graduate students.

### 2.1.1 The Ly $\alpha$ forest as a tracer of structure

The Ly $\alpha$  forest of absorption features due to neutral hydrogen can be seen in the spectra of both quasars Rauch (1998) and galaxies (e.g., Savaglio et al. (2002)). We refer to quasars and galaxies as “backlights” rather than “sources” in what follows, in order to avoid confusion with the “sources” in gravitational lensing (which will be the Ly $\alpha$  forest here). At the redshifts ( $2 < z < 6$ ) where the Ly $\alpha$  transition is in the optical wavelength range, the forest absorption mostly arises in the moderately overdense (of order the cosmic mean) intergalactic medium (IGM) (Bi (1993), Cen et al. (1994), Zhang et al. (1995), Hernquist et al. (1996)). This intergalactic medium is a continuous field, and as such Ly $\alpha$  forest spectra can be thought of as a collection of one-dimensional “intensity maps”, where the relevant property is the “flux overdensity”,  $\delta_F = \frac{F}{\langle F \rangle} - 1$  ( $F$  is the transmitted flux in a spectrum). Its properties are well studied and it is relatively easy to simulate numerically (see e.g., Bolton et al. (2017)). The forest has been used to test cosmological models, for example through the influence of the neutrino mass on large-scale structure (e.g., Palanque-Delabrouille et al. (2015), Croft et al. (1999)). With a high enough angular density of quasars, three dimensional statistics can be evaluated by using information from multiple sightlines, enabling clustering measurements and detection of baryon oscillations (Busca et al.). The collection of one-dimensional skewers can also be used to make continuous three dimensional maps using a variety of interpolation techniques (e.g., Cisevski et al. (2014)), and with even more numerous star forming galaxies as background spectra these can be made with angular resolution close to arcminute scales (Lee et al., 2014).

The Ly $\alpha$  forest, being measured from spectra has a precisely known source redshift. This fact is also advantageous for lensing of the CMB, enabling analyses to be free of uncertainties in the redshift distribution of sources which affect galaxy weak lensing studies (Hearin et al., 2010).

### 2.1.2 Lenses for the forest

The Ly $\alpha$  forest at redshift  $z_s$  is lensed by the matter distribution lying between us and  $z_s$ . Gravitational lensing shifts the observed positions of points on the sky without changing their surface brightness. In the case of the Ly $\alpha$  forest, this means that the quasar or galaxy backlights move on the plane of the sky. The angular sizes of quasars are magnified (through the change in their angular sizes). This magnification of quasars through lensing is well studied, from the first observed lenses, which created multiple quasar images (Walsh et al., 1979), through weak lensing magnification of quasars detected by cross-correlation with foreground galaxies (e.g., Scranton et al. (2005)). The magnification of quasars will cause some selection biases which we plan to investigate with mocks. Directly relevant to Ly $\alpha$  forest lensing, however are distortions of the angular separations between quasars, caused by the lensing deflection of light. Gravitational lensing therefore distorts the “image” of the IGM probed by the Ly $\alpha$  forest without changing the transmitted flux measured in each pixel. This is directly analogous to the effect of lensing on 21cm emission (or the CMB), which conserves surface brightness. In the left panel of Figure 2 we illustrate this with a diagram, which shows the Ly $\alpha$  forest pixels being deflected in a similar fashion to the quasar backlights. In the right panel of Figure 2 we concentrate on a single backlight and Ly $\alpha$  forest pixel and show the relationship to the unlensed angular

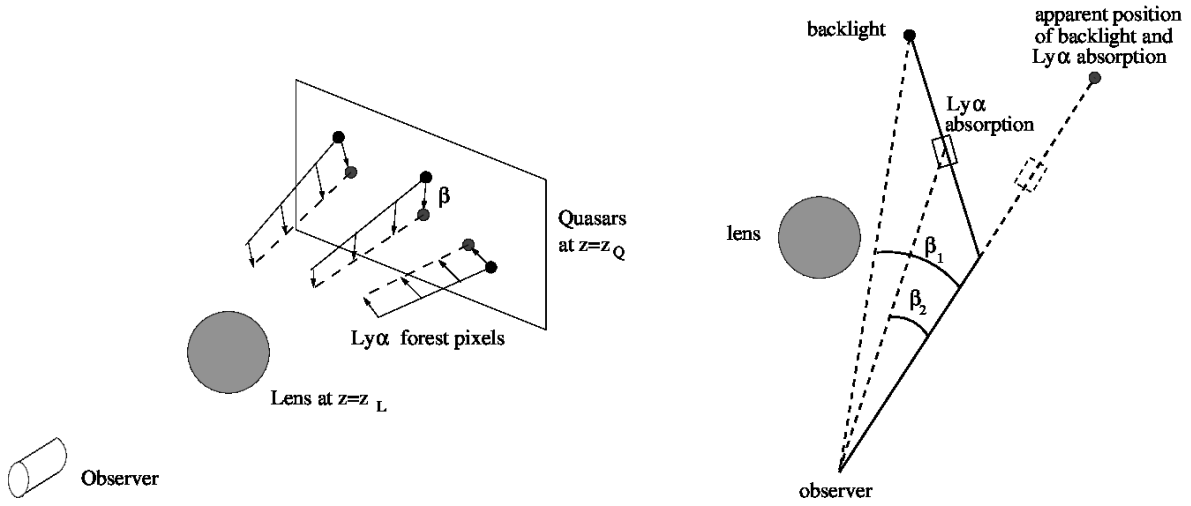


Figure 2: **Left panel: cartoon illustration of the geometry of Ly $\alpha$  forest lensing.** Due to lensing by the foreground object at redshift  $z_L$ , the angular position of a quasar at redshift  $z = z_Q$  is deflected by an angle  $\beta$ . The associated Ly $\alpha$  forest pixels are also lensed, deflected by an angle smaller than  $\beta$  (which depends on the angular size distance to the absorption in the pixel). **Right panel: lensing deflection for a single Ly $\alpha$  forest pixel.** The deflection angle for the backlight ( $\beta_1$ ) is different from that for the Ly $\alpha$  forest absorption ( $\beta_2$ ) because they are at different redshifts (and therefore angular size distances).

positions of both. The pixel and the backlight are at different angular size distances, and so are displaced on the sky by different angles.

If the lensing deflections are small compared to structure in the source, the Ly $\alpha$  forest flux overdensity  $\delta_F$  at wavelength  $\lambda$  can be expressed as a Taylor expansion of the unlensed  $\delta_F$ .

$$\tilde{\delta}_F(\boldsymbol{\theta}, \lambda) = \delta_F(\boldsymbol{\theta} - \boldsymbol{\alpha}(\boldsymbol{\theta}), \lambda) \simeq \delta_F(\boldsymbol{\theta}, \lambda) - \boldsymbol{\alpha}(\boldsymbol{\theta}) \cdot \nabla_{\boldsymbol{\theta}} \delta_F(\boldsymbol{\theta}, \lambda) + \dots \quad (3)$$

This expansion is valid in the case of the Ly $\alpha$  forest, where gradients in  $\delta_F$  can be large, but the deflections (or deflection gradients) are small compared to them on all scales of interest. The deflection field  $\boldsymbol{\beta}(\boldsymbol{\theta})$  is related to the 2D projected lensing potential via  $\nabla \Phi = -\boldsymbol{\beta}(\boldsymbol{\theta})$ , in the weak lensing limit. This lensing potential can be computed from the full 3D gravitational potential (e.g., Bartelmann & Schneider 2001) by an integration over redshift as in Eq. (1). This lensing potential can be reconstructed from the Ly $\alpha$  forest field using quadratic estimators (e.g., Hu and Okamoto (2002)).

## 2.2 Galaxy Clustering

### 2.2.1 The Effect

The simplest statistic that characterizes the angular distribution of galaxies on the sky is the angular correlation function,  $w(\vec{\theta}_1, \vec{\theta}_2)$ , which quantifies the excess probability over random that a galaxy will be found at  $\vec{\theta}_2$  given that there is a galaxy at  $\vec{\theta}_1$ . In the isotropic case, the angular correlation function depends only on the angular distance between the two positions:  $w = w(|\vec{\theta}_1 - \vec{\theta}_2|)$ . The ATF effect here means that  $w$  depends also on the location on the sky.

This is simplest to envision and to measure when measuring  $w$  behind a massive object such as a galaxy cluster. Fig. 3 shows a schematic picture of this. For example, the positions of the two galaxies directly to the left of the cluster are deflected by different amounts (the one closest is deflected more than the one further away, so the observed distance between those two galaxies is *smaller* than it would be in the absence of lensing. The observed  $w$  then is governed by the larger unlensed distance. Walking through this exercise for all pairs of galaxies in the picture make it clear that the observed  $w$  will not depend on simply the observed

angular distance between pairs of galaxies. Indeed, we argue that **the most impactful implementation of the ATF of galaxies will be to measure the masses of galaxy clusters.**

### 2.2.2 Context

Galaxy clusters are the largest, most massive bound structures in the universe and therefore are the key to a number of cosmological puzzles. Chief among these is identifying the mechanism responsible for the current epoch of cosmic acceleration. The community has moved on from simply measuring the equation of state of a hypothetical dark energy substance. There is now a concerted effort to test the canonical  $\Lambda$ CDM predictions both for the expansion history of the universe and for the rate of the growth of structure. Galaxy clusters offer the potential for testing both of these predictions: the number of rare objects such as clusters at a given time is exponentially sensitive to the RMS fluctuations in the density field, so cluster abundance at multiple redshifts can be translated into measurements of the growth function. Similarly, the abundance is sensitive to the volume of a given redshift slice, which depends on the redshift-distance relation.

The one impediment to date of using clusters as a powerful tool is the uncertainty in cluster masses. However, we are entering an exciting epoch that promises to change this situation. Besides the large surveys now online and coming online in the 2020's, five ways of inferring cluster masses have emerged and using all of them together leads to the hope that the systematic uncertainties in any one of them will not induce a large bias. The techniques of interest are: cluster richness, X-Ray luminosity, Sunyaev-Zel'dovich signal induced by hot electrons in the intracluster gas, weak lensing by galaxies, and most recently weak lensing by the cosmic microwave background (CMB) Liu et al. (2015); Baxter et al. (2015); Zu et al. (2014); Melchior et al. (2017); Simet et al. (2017); Baxter et al. (2017). This proposal aims to add yet another tool that can measure galaxy cluster masses. Dodelson has not only helped launch the field of CMB cluster lensing with Baxter et al. (2015), but also serves as Co-Chair of the Dark Energy Survey Science Committee. He brings insight into the DES cluster cosmology analysis. The Year 1 analysis will be released by the time this proposal is read, and we are currently working on Year 3 data. From the estimates below, it is possible that ATF of galaxies will emerge as a powerful tool for cluster cosmology even for DES data. The situation is even more promising for next generation surveys, such as LSST.

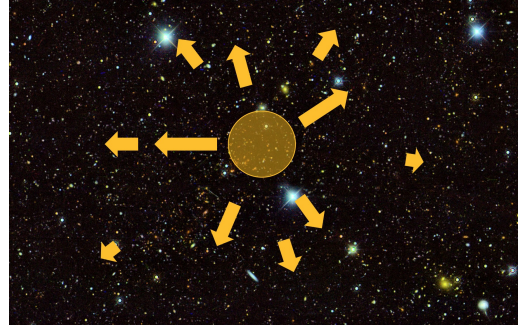


**Figure 3: Cartoon of the impact of a foreground lens on background galaxies.** All galaxies appear further away from the cluster center, their observed positions shifting as indicated by the arrows. Galaxies closest to the center experience the largest shift in position (this lensing deflection is not shown to scale). The correlation function of the background galaxies will also be distorted by these deflection angles, and this is what we plan to measure.

### 2.2.3 Signal to Noise

Let us provide a rough estimate of the detectability of the ATF of the galaxy distribution due to a typical cluster of mass  $2 \times 10^{14} M_{\odot}$ . We can assume that the unlensed  $w(\theta)$  is known extremely well because it can be measured over the large area covered by any modern survey (e.g., in DES, this is 5000 square degrees and 20,000 in LSST). The observed correlation function of the background galaxies will be distorted due to the presence of the foreground lens, as in the cartoon in Fig. 3. Each galaxy's position will be shifted:

$$\vec{\theta}^{\text{obs}} = \vec{\theta} + \vec{\delta\theta}(\vec{\theta}) \quad (4)$$

where  $\vec{\theta}$  is the undeflected position, and the deflection angle  $\vec{\delta\theta}$  is a function of  $\vec{\theta}$  that depends on the mass distribution of the lens. For the purpose of this estimate, we assume a point mass lens,

$$\vec{\delta\theta}(\vec{\theta}) = \vec{\theta} \frac{\theta_E^2}{\theta^2}. \quad (5)$$

For a lens a typical distance of 1 Gpc from us (and sources far behind), the Einstein radius  $\theta_E = 40''(M/2 \times 10^{14} M_\odot)^{1/2}$ .

The unlensed positions are  $\vec{\theta}^{\text{obs}} - \vec{\delta\theta}$ , and the correlation function governing those unlensed positions is  $w(\theta)$ . Therefore, the observed angular correlation function between two positions  $\vec{\theta}_i$  and  $\vec{\theta}_j$  is

$$w^{\text{obs}}(\vec{\theta}_i^{\text{obs}}, \vec{\theta}_j^{\text{obs}}) = w(|\vec{\theta}_i^{\text{obs}} - \vec{\delta\theta}(\vec{\theta}_i) - \vec{\theta}_j^{\text{obs}} + \vec{\delta\theta}(\vec{\theta}_j)|). \quad (6)$$

For the purposes of estimating the magnitude of this effect, we now make the approximation that the deflections are small, so the argument of  $w$  on the right-hand side can be Taylor expanded. Note that this approximation is not essential, as in the case of CMB cluster lensing Baxter et al. (2015) we avoided it by using a likelihood approach, but this will be the first step in our program. Taylor expanding and dropping the  $^{\text{obs}}$  superscript on the angles leads to

$$\begin{aligned} w^{\text{obs}}(\vec{\theta}_i, \vec{\theta}_j) &= w(\theta_{ij}) + w'(\theta_{ij}) \left[ \vec{\delta\theta}(\vec{\theta}_i) - \vec{\delta\theta}(\vec{\theta}_j) \right] \cdot \frac{\vec{\theta}_i - \vec{\theta}_j}{|\vec{\theta}_i - \vec{\theta}_j|} \\ &\equiv w(\theta_{ij}) + w'(\theta_{ij}) f_{ij} \end{aligned} \quad (7)$$

where here  $\theta_{ij} \equiv |\vec{\theta}_i - \vec{\theta}_j|$ ;  $w' \equiv dw/d\theta$ , which can be measured extremely accurately from all other patches in the survey; and the second line condenses the additional terms to save space.

The second term in Eq. (7) is the effect we are after, the signal, as it contains the information about the deflection angles that depend on the mass of the lens. To estimate the signal to noise, we imagine pixelizing the region around the lens and forming an estimator for the angular correlation function for every pixel pair:

$$\hat{w}(\vec{\theta}_i, \vec{\theta}_j) = \delta_i \delta_j \quad (8)$$

where  $\delta_i \equiv (n_i - \bar{n})/\bar{n}$ . Here  $n_i$  is the number of galaxies in pixel  $i$  and for simplicity it is assumed that the expected number of galaxies in each pixel is equal to  $\bar{n}$  (i.e., it is assumed that the mask is trivial). This is the Landy and Szalay (1993) estimator, with an expectation value equal to Eq. (7). As a first estimate, we neglect cosmic variance, so that the error on the estimator is simply Poisson noise:

$$\text{Var}(\hat{w}) = \frac{1}{\bar{n}^2}. \quad (9)$$

The signal to noise squared then is

$$\left( \frac{S}{N} \right)^2 = \sum_{ij} \frac{(w'(\theta_{ij}) f_{ij})^2}{1/\bar{n}^2}. \quad (10)$$

To make an estimate of the signal to noise, we need to insert information about the angular correlation function and the background galaxy density. For these purposes, we follow Section 9 of the LSST Science Book and assume

$$w(\theta) = 0.36 \left( \frac{1'}{\theta} \right)^{0.8} \frac{0.1}{\Delta z}. \quad (11)$$

As an estimate of the current capabilities, we take the source galaxies in DES in the redshift bin  $0.6 < z < 0.9$  with their number density of 1.5 per square arcminute. As a sanity check, the slope and amplitude in Eq. (11) are consistent with the latest DES measurements (Elvin-Poole et al., 2018) when projected to the source galaxy redshift width and bias. In this simple example of a point mass, the signal falls off rapidly, so the estimate excludes regions close to the center to be conservative (these are the regions most likely to be impacted by contamination from cluster galaxies), but more realistic profiles will likely get more of the signal from galaxies out to radii similar to those used for shapes ( $\sim 5'$ ). The key advantage of this technique is that the signal depends on the number of pairs, so the signal to noise scales as  $n$  not as the shape measurements, which scale as  $n^{1/2}$ ,

The results of this estimate are that **the expected signal to noise is large**. Even for a current survey like DES, the signal to noise from a single tomographic bin with  $0.6 < z < 0.9$ , the expected signal to noise behind

a single cluster is 0.3. Therefore, stacking only 1000 clusters (the Year 1 catalog has closer to 10,000) leads to a 10% mass determination. With its more precise photometric redshifts and larger background galaxy density, **LSST could measure the mass of a single cluster with 10% uncertainty** using the ATF technique.

Of course this estimate needs to be fleshed out and tested on simulations; indeed, this is the main aim of a large part of the proposal (§3).

## 2.3 Time Delays

Photons that comprise the CMB experience time delays or advances depending on the integrated potential through which they travel, as depicted in Fig. 4. Since photons do not decouple instantaneously from the electron-proton plasma, the surface of last scattering is often said to have a finite width; however, the directional-dependent change in the distance to last scattering is independent of its finite width and is also different than the angular deflections that have been captured by recent experiments.

The integrated potential that determines the time delays differs from the one that cause the deflections, so if we can measure time delays, we will have measured a new cosmic field. As an estimate of how viable this is, we follow the formalism of Hu and Okamoto (2002) and to obtain estimators that are quadratic in the CMB fields (temperature and two components of polarization). As an example the relevant estimator quadratic in temperature is

$$\hat{d}_{LM} = B_L \sum_{l_1 m_1} \sum_{l_2 m_2} (-1)^M \begin{pmatrix} l_1 & l_2 & L \\ m_1 & m_2 & -M \end{pmatrix} h_{l_1 l_2}(L) T_{l_1 m_1}^{\text{obs}} T_{l_2 m_2}^{\text{obs}} \quad (12)$$

where the sum is over two angular momenta that can combine to form  $LM$  and  $h$  is a coefficient that depends on the *radial derivative* of the CMB power spectrum with respect to the distance to the last scattering surface:  $\partial C_l / \partial \ln(D_*)$ . This spectrum is depicted in Fig. 5.

The estimator in Eq. (12) has an expectation value equal to the fractional difference in distance along the line of sight (actually the coefficients of that fractional distance field decomposed into spherical harmonics). Similarly, we can form estimators for combinations of the temperature and the two polarization fields and combine all estimators to estimate the signal to noise. Preliminary estimates point to the possibility of detection, but only with next generation surveys. We propose to develop these estimators to obtain reliable projections accounting for systematics. These projections can help inform the design capabilities of a survey such as CMB-S4. As described below, we also will work on the possibility of detecting time delays of the CMB behind galaxy clusters; i.e., in cross-correlation. Another possibility is to estimate not the power spectrum of the time delay field but rather the cross-spectrum of the deflection field (which has a larger amplitude) with the time delay field. In short, time delays offer exciting opportunities to open up new horizons in CMB analysis.

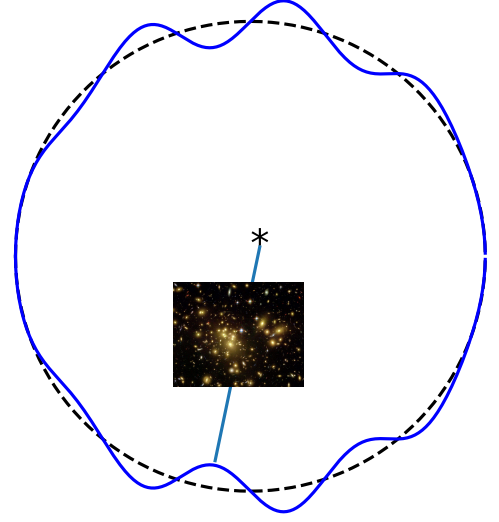


Figure 4: Schematic of the impact of time delays on the last scattering surface with us at the center. Dashed line denotes the assumed spherical last scattering surface, while blue solid curve denotes the more realistic corrugated surface due to time delays. Rays that pass through over-dense regions (as depicted in the figure) are slowed down; since all photons were released from the electrons at the same time, these “slower” photons travel shorter distances and therefore originated from closer distances than average.

## 3 Planned work: Simulations and mock catalogs



We will carry out a significant portion of our research using simulations and mock catalogs. For the forest lensing we will build on our successful linear theory tests (C18). For galaxy clustering, we will use many of the same simulations and tools. First, we will refine the estimate in §2.2 by accounting for: cosmic variance as an additional source of noise (although this should not have too large of an impact on the small scales of interest), more realistic cluster profiles including mis-centering, the impact of magnification, the validity of the Taylor expansion, optimal angular binning, and photometric red shift errors and binning.

Unlike CMB lensing, the assumption of an initially Gaussian *source* field is not a good one for the first two of our weak lensing tracers. The foreground lens density field is also at lower redshift than in the CMB case, meaning that the *lens* density fluctuations will also be further into the non-linear regime. Mock observations that include these non-linearities are therefore crucial to test our methods. We will be working with a set of already run simulations as well as carrying out some new ones to set up a comprehensive set of realistic tests of lensing reconstruction and measurement. In this section of the proposal we outline how we plan to do this, starting with the raw N-body and hydro simulations. In Table 1 we list some of the privately run simulations available to the project. We will also make use of public simulation datasets such as Giocoli et al. (2016) to supplement them.

| Run                       | $N_{\text{part}}$ | $L_{\text{box}}$<br>(Mpc/h) | $\epsilon$<br>(kpc/h) | $z_f$ | Physics                    |
|---------------------------|-------------------|-----------------------------|-----------------------|-------|----------------------------|
| <i>MassiveBlack-II</i>    | $2 \times 1792^3$ | 100                         | 1.85                  | 0     | DM, Gas, Stars, Blackholes |
| <i>MassiveBlack-II DM</i> | $2 \times 1792^3$ | 100                         | 1.85                  | 0     | DM (complete)              |
| <i>Lyman-alpha</i>        | $2 \times 4096^3$ | 400                         | 10.0                  | 1.5   | DM, Gas, Stars             |
| <i>BlueTides DM</i>       | $2 \times 1758^3$ | 400                         | 6.00                  | 0     | DM                         |
| <i>Zhu et al. DM</i>      | $1024^3$          | 1000                        | 10.00                 | 0     | DM, 20 realizations        |

Table 1: **N-body Simulations available to this project.** The columns denote the runs, the number of particles  $N_{\text{part}}$ , the size of the simulation box  $L_{\text{box}}$ , the gravitational softening length  $\epsilon$  and the final redshift to which it was run  $z_f$ . The last column denotes the physics involved.

### 3.1 Ly $\alpha$ source field

Relevant Ly $\alpha$  forest pixels for lensing will be mostly between redshifts  $z = 2 - 3.5$ , with the lower end of the range due to the atmospheric cutoff and the upper due to the decreasing availability of bright quasars and galaxies. Simulating the forest involves resolving scales as small as the pressure smoothing scale ( $\sim 100\text{kpc}$ , Peebles et al. (2010)) while incorporating large scale modes on scales of tens of  $h^{-1}\text{Mpc}$ . We will model the forest using the following three techniques which have different strengths.

#### 3.1.1 Lognormal models

In order to cover the largest volume, and make contiguous source fields with diameters spanning large fractions of the sky (relevant for surveys such as eBOSS and DESI), we will use lognormally transformed linear density fields. This technique was introduced by Bi and Davidsen (1997) and has been shown to be a good approximation to full hydrodynamic simulations for purposes such as measuring baryonic acoustic oscillations Le Goff et al. (2011). Large-scale velocity fields will be included via the Zeldovich approximation, and thermal broadening added via a temperature density relation Keating et al. (2017).

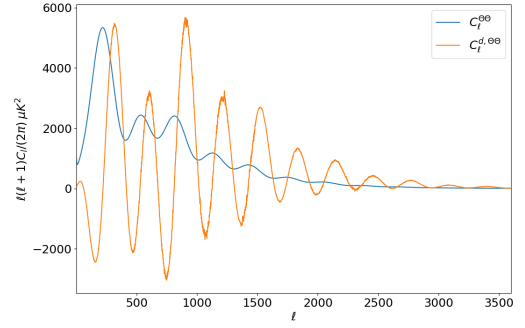


Figure 5: The standard CMB temperature power spectrum  $C_l^{\Theta\Theta}$  compared to the one that is used in the estimator to extract time delays:  $C_l^{d,\Theta\Theta} \equiv \partial C_l / \partial \ln(D_*)$ .



### 3.1.2 Hydrodynamic simulations

Full hydrodynamic simulations will be useful to capture the effect of small scale density fluctuations. Although volumes are relatively smaller than what can be achieved with lognormal fields, the differences stemming from full simulation in lensing measurements from individual small areas will be measured without cosmic variance by comparing the hydro simulations directly to lognormal fields with the same random phases. The PI has run a  $400 h^{-1} \text{Mpc}$  simulation (used in Cisewski et al. (2014)) with the Gadget-3 SPH code with full hydrodynamics, and this will be available to this project. The volume spans 5.5 degrees at  $z = 2.5$  and this is enough to simulate surveys several times larger than CLAMATO. Other simulations are available with additional physics activated (see Table 1) including star formation and black holes.

By mapping sections of hydrodynamic simulations onto a much larger dark matter simulation (or even linear density fields) it is possible to accurately reproduce many of the features of the  $\text{Ly}\alpha$  forest in a larger hydrodynamic simulation. This technique was used successfully by Croft (2004) and developed in detail by Peirani et al. (2014). We have all the relevant simulation ingredients and will adopt this approach as well.

## 3.2 $\text{Ly}\alpha$ forest source Mocks

$\text{Ly}\alpha$  forest spectra will be made by integrating through the neutral hydrogen distribution (in SPH kernels in the case of the hydro simulations) along each sightline and then convolving with the line-of-sight velocities and applying thermal broadening (Hernquist et al., 1996). In order to make realistic mock catalogs we will use the relevant observational parameters of different datasets from Table 2. Quasar and galaxy sightlines will be picked randomly with the correct mean spacing. In our test so far (C18) we have used a grid of background sources, which is obviously unrealistic, and so an important part in our proposed work is to abandon that simplification. Apart from survey geometry we will investigate the role of uncertainties in quasar and galaxy continua. We will apply continua based on published principal components of quasar spectra (Lee et al., 2013) and population synthesis models to the mocks, before fitting them using low order polynomials. This will enable us to estimate the covariance between pixels on large-scales which are due to continuum fitting.

## 3.3 Galaxy sources

In our study of ATF of galaxies it is important to resolve large-scale structure in the galaxy distribution but galaxy shapes themselves are not needed. A number of suitable N-body simulations are therefore available to use, for example those used in Zhu et al. (2017b) (see Table 1, and we will use a HOD approach (e.g.) to populate the dark matter distribution with galaxies. Although angular clustering will be measured, we will make use of the three dimensional information in the simulations to assign photometric redshifts and model systematic uncertainties related to their use in the presence of errors, catastrophic and otherwise (Hearin et al., 2010). Hydrodynamic simulations of small volumes are also available (Table 1) and will be used as the source fields in lensing simulations of individual galaxy clusters in order to investigate baryon physics effects.

## 3.4 CMB time delay source field

Our main aim with the CMB time delay lensing probe is to make predictions for what will be possible with CMB S4 instruments. We will therefore simulate full sky CMB fields using HEALPix, as well as plane parallel source mocks which will be placed behind clusters in the lens simulations (below)

## 3.5 Simulated lenses

In situations such as forest lensing with widely spaced sightlines, the lensing field will be detected only on large angular scales where the matter structure responsible for the lensing is linear to a reasonably good approximation. Our lens simulations (e.g. C18) have started from the simplest case, a Gaussian random field. We create a realization of the lensing potential by generating random Gaussian distributed Fourier modes with

the power spectrum expected in the same cosmology used to simulated source fields. The deflection is found by taking the gradient of the potential using an FFT. Points on the source planes are then displaced by the deflection to get the lensed image. In the case of the forest, the deflection is applied to individual pixels (see Figure 1) in the forest source simulations and for ATF of galaxies to the galaxies described in Section 3.3 We will start with a single lens plane approximation for the forest lensing case based on the linear fields. For the ATF with a cluster lens, the simplest initial simulations will be of a single spherically symmetric lens.

In order to capture the true non-linearity inherent in the lens field, we will then move to using ray-traced Nbody simulations. We have chosen GLAMER Metcalf and Petkova (2014) to do this (collaborator Ben Metcalf is an author of the code). It incorporates adaptive mesh refinement for efficient choice of ray shooting. The deflection and beam distortions (convergence and shear) are calculated by modified tree algorithm when haloes, point masses or particles are used and by fast Fourier transform when mass maps are used. The combination of these methods allow for a very large dynamical range, so that accurate maps will be made spanning several degrees and covering large-scale structure in the lensing matter distribution. Multiple lens planes can be handled by GLAMER Petkova et al. (2014), and the distribution of matter will be taken from the simulations detailed in Table 1. A suite of publicly available raytraced simulations (the Multi Dark Lens Simulations, Giocoli et al. (2016)) has been carried out and will also be used for this project. These include over 150 realizations of  $\sim 10$  square degree fields carried out using fully sampled lightcone raytracing with 24 lens planes each. The simulations therefore cover both the redshift  $z > 1$  lenses relevant for CMB time delay and forest lensing and the lower redshift needed for galaxies in the same simulation. They can be used to test both, and in principle look at the overlap in lensing reconstruction (and lensing kernels) for the two methods.

### 3.6 Full mocks

Given the simulated sources and lens described above, we will construct full mock datasets where we mimic the geometry and noise properties of particular datasets. These datasets are detailed below in Section 6. We note that because some of them are extremely large in angular extent (e.g. eBOSS and DES), we will make use of a combination of small high fidelity mocks of sections (for example individual galaxy clusters) and others larger areas generated using the approximate techniques mentioned above. We will also incorporate addition levels of complexity and potential sources of systematic error, treating the addition of each in turn. Magnification will be important, as both source galaxies and background quasars will be selected preferentially when they are lensed. The effects of photometric redshift uncertainties could also be added at this stage.

## 4 Planned work: Estimators

Reconstructing the lensing mass distribution from observations (and making maps, or measuring clustering statistics or object properties directly) requires an estimator. A quadratic lensing estimator (e.g., Hu and Okamoto (2002)) for the forest or for LIA is sensitive to variations in the power spectrum in different regions of the sky. These spatial variations result in correlations in Fourier modes (or  $C_\ell$ 's) that would not exist otherwise. In our proposed work, we will further develop estimators of the type that have been applied to the CMB but specialized to our new tracers (for example the discrete sightlines of the Ly $\alpha$  forest).

### 4.1 Estimators for anisotropic galaxy clustering

In the case of ATF of galaxies we will be concentrating first on detecting and measuring the lensing signal of stacked galaxy clusters.. The simplest estimator to try first is a parametric model with, e.g., the mass and concentration of the clusters set as free parameters. The data points will be  $N_{\text{pix}}^2/2$  estimates of  $\hat{w}$ , and these can be used to constrain the parameters. We will also explore maximum likelihood methods that do not rely on the small angle approximation.

## 4.2 Estimators for Ly $\alpha$ forest lensing

In C18 it was found that the standard quadratic estimator works very well on gridded spectral Ly $\alpha$  forest data. As real galaxies and quasars do not exist on a grid, the challenge is to develop an estimator that works on a random discrete set of sightlines. Several different approaches can be taken, the simplest being an interpolation of the data onto a finely spaced uniform grid. We have experimented with this approach, finding that it could be useful in conjunction with the detailed simulation tests proposed above to establish how interpolation errors propagate. However, the PI, together with collaborator Ben Metcalf has developed a quadratic estimator which uses non-gridded data (Metcalf et al. (2018)). Without a grid, FFT methods are not available to speed up the estimator, but inversion of large matrices is required. At present tests on small (million pixel) simulations have shown success and during this proposal we will improve the code and scale up to the capabilities needed to process full mock and observational datasets.

## 4.3 Mitigating systematics: the road to precision cosmology

Our simulation tests with realistic sources and lens fields will reveal the extent to which non linearity and non Gaussianity affect the lens reconstructions. We will seek to develop methods to mitigate these effects. For example, in CMB lensing Lewis and Pratten (2016) have shown how the effects of non Gaussian deflections from post-Born corrections and non-linear structure growth can be severely reduced by Gaussian smoothing. Also for CMB lensing, Böhm et al. (2018) have shown that results from raytraced simulations can be accounted for and corrected using analytic results (Böhm et al. (2016)). Although in the CMB these issues are at the  $\sim 0.3\%$  level in the power spectrum, they will be a more significant issue with our lower redshift lensing tracers and should be addressed as we seek to develop them as new tools for precision cosmology. We will use the CMB lensing work as a guide to push the precision of our work to below the level of the simulated systematics.

## 4.4 Cross-correlation and validation

As our lensing techniques are new, an important part of our studies will be checking results against relevant prior data. Measurement of cross-correlations with foreground galaxies or CMB lensing maps are likely to constitute the first proof that our techniques are valid. In the case of forest lensing, foreground galaxy maps are available for large areas of the sky from the SDSS/BOSS and eBOSS surveys. We can use the distribution of galaxies (LRGs and ELGs from eBOSS) with redshifts, weighted by the lensing kernel to make a predicted lensing convergence map. We will cross-correlate this map with convergence estimated from the forest. We will test this cross-correlation with our mock catalogs, and use them to quantify systematic errors. In the case of LIA galaxy clusters selected from photometry itself play the largest role, and again the mocks will be important to bracket uncertainties (such as the role of baryonic physics Zentner et al. (2013)).

# 5 Planned work: Observational measurements

The new weak lensing tracers we are proposing are unusual in that observational data already exists which could allow high significance detections and precise constraints on cosmology. We therefore plan to move rapidly to make first detections alongside our work on mock catalogs, using those mocks to inform our estimates of errors and uncertainties.

## 5.1 The CLAMATO survey: first detection of Ly $\alpha$ forest lensing

The COSMOS Lyman-Alpha Mapping And Tomography Observations (CLAMATO, Lee et al. (2018)) survey is a dense sampling of Ly $\alpha$  forest spectra in the COSMOS field, using both quasars and galaxies as backlights. Some characteristics of the survey are given in Table 2. The sightline density is such that one can expect

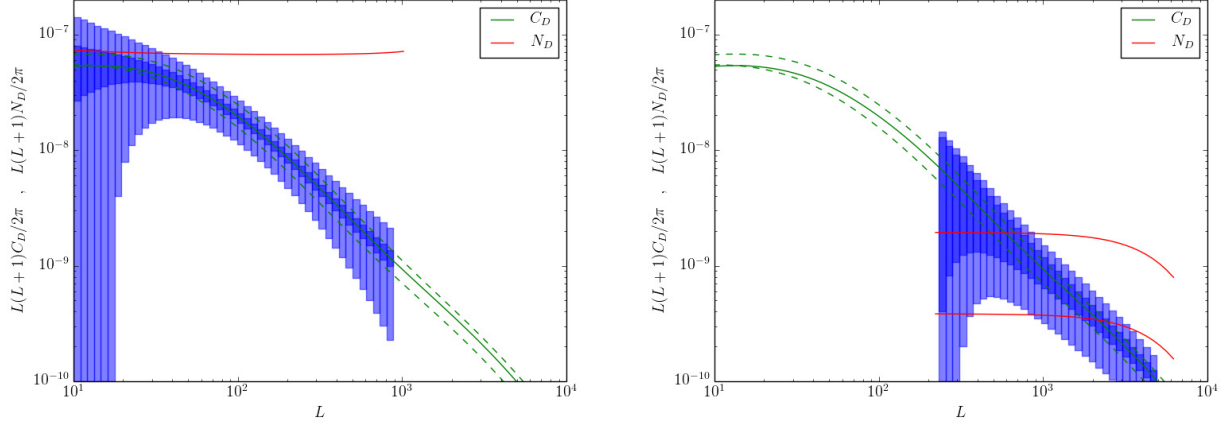


Figure 6: **The predicted lensing displacement power spectrum measured from the Ly $\alpha$  forest and its estimated errors.** **Left panel:** eBOSS survey (see Table 2). The smaller errors are for a redshift range  $\Delta z = 0.5$  and the larger for  $\Delta z = 0.1$ . For this survey,  $N_D$  (the noise per mode, red line) is off the range of the plot. The green curves labelled  $C_D$  show the expected power spectra, with the solid curve being for  $z_s = 2.5$ . For comparison, the upper dashed green curve shows results for  $z_s = 3$  and the lower one for  $z_s = 2$ . **Right panel:** The CLAMATO survey (2). The two red curves are the noise in each mode,  $N_D$ , for the  $\Delta z = 0.5$  (lower) and  $\Delta z = 0.1$  (higher) cases. Where  $N_D$  is below  $C_D$  high fidelity maps of the lensing convergence is possible.

| Dataset   | When      | Area            | N'spectra | mean separation |
|-----------|-----------|-----------------|-----------|-----------------|
| BOSS DR12 | 2016      | 10,000 sq. deg. | 160,000   | 15 arcmin       |
| eBOSS     | 2014-2020 | 7,500 sq. deg.  | 270,000   | 10 arcmin       |
| CLAMATO   | 2014-2020 | 0.8 sq. deg.    | 1,000     | 1.7 arcmin      |

Table 2: **Ly $\alpha$  forest observational datasets we will use.** Of these, BOSS (Dawson *et al.* 2013) has been completed, eBOSS (Dawson *et al.* 2016) and CLAMATO (Lee *et al.* 2014, using galaxy spectra) are ongoing.

to make high fidelity maps of the foreground lensing mass once the survey is completed. An approximate idea can be gained from Figure 7 where we show tests of the reconstruction technique from C18 where the sightline density was similar to that in the CLAMATO survey. CLAMATO has had its first public data release Lee *et al.* (2018) and we will use this data to make what is likely to be the first detection of Ly $\alpha$  forest lensing. A prediction of the signal to noise expected in a determination of the lensing mass power spectrum (taken from the PI's work Metcalf *et al.* (2017)) is shown in Figure 6. For the full survey we expect an 6 % constraint on the amplitude of mass fluctuation  $\sigma_8$ . The first data release contains about one third of the hoped for final dataset. Galaxy densities are available to high redshift in the COSMOS field meaning that validation of the measurement with cross-correlation should be straightforward.

## 5.2 eBOSS: 3 percent precision on $\sigma_8$

The eBOSS survey is ongoing, but has completed more than two thirds its survey footprint and will be complete early in our project. It is a large area, low sightline density survey (see Table 2), so that foreground mass maps will have low fidelity. The large area will however lead to a precise measurement of the power spectrum. The right panel of Figure 6 shows our prediction from Metcalf *et al.* (2017), which yields a 3% measurement of  $\sigma_8$ .

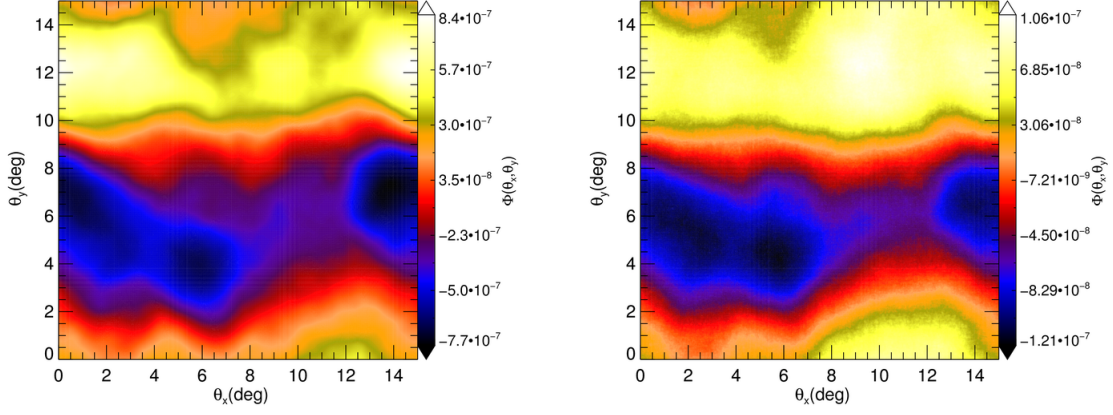


Figure 7: **Recovery of the lensing potential field from a simulation of Ly $\alpha$  forest lensing.** The left panel shows the input potential and the right panel the potential reconstructed from a lensed Ly $\alpha$  forest dataset. The plot is taken from C18, and used gridded forest data (something which will be improved in our proposed work). The mean spacing of sightlines was comparable to that in the CLAMATO survey, which we plan to analyze.

### 5.3 DES clusters: precision stacked cluster mass profiles

Once tested on simulations, we will apply our ATF method to clusters in the Dark Energy Survey Dark Energy Survey Collaboration et al. (2016), for which the Co-I is co-Chair of the Science Committee. As we have shown in Section 2.2, high signal to noise will be available given that even the year one catalog contains tens of thousands of galaxy clusters that are selected using the redMaPPer algorithm Melchior et al. (2017). Indeed, the amplitude of the stacked cluster profile from year 1 DES data will have a statistical precision of 1.5%, easily in the regime where systematic errors of all methods (such as shear and lensing magnification) are important, showing that a new method will be extremely valuable. Along these lines, comparison will be made to the shear-based mass measurements of the same clusters Simet et al. (2017) and with estimates of their mass inferred from the angular clustering of clusters themselves Baxter et al. (2016). The estimator codebase developed and used on DES data will be released to the community so that it can be used, for example, by all members of the LSST Dark Energy Science Collaboration.

## 6 Broader impact and outreach

The best outreach program should be able to easily reach women and minority groups underrepresented in science. Video games provide a good way to do just that- a study from the Pew Internet & American Life Project (Lenhart 2008) found that the percentage of American youth that play video games is almost the same for a wide range of racial and ethnic groups and incomes. The survey combined the telephone responses from a nationally representative sample of 1,102 young people, ages 12 to 17, and their parents. It found that 99% of boys and 94% of girls play video games, and they play them often, with half of the respondents saying they had played a video game the previous day. This adds up to over 200 million person-hours of video gaming each day in the U.S.

Games are clearly entertaining as judged by their use, but what if they had educational benefits? Our proposal focuses not on general computer and video games, but on educational games, and the ideas we incorporate are grounded in a theory of intrinsically motivating instruction based on a rigorous study of educational games (Malone 1981, Gee 2003, Squire 2003, Aldrich 2004, Schell 2008).

Through the medium of games, our outreach aims are the following:

(1a) To introduce elementary and middle school students to the length scales relevant to astronomy, from the Solar system to the large scale structure of the Universe .

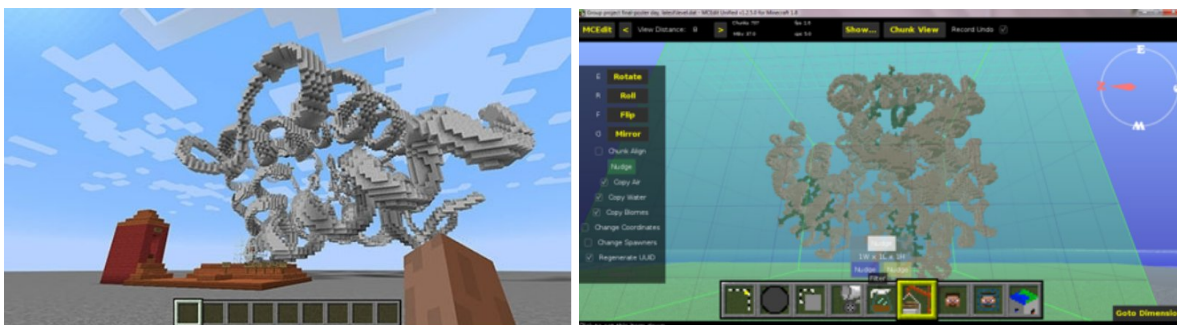


Figure 8: **Left: Minecraft visualization of myoglobin molecule** Reproduced from the MolCraft project, University of Hull, UK **Right: Importing three dimensional structure into Minecraft using MCedit** Reproduced from the MolCraft project, University of Hull, UK

(1b) To introduce school children to the chemical constituents of the Universe and how they are distributed on Astronomical scales.

(1c) To introduce high school students to the concept of quasars, the intergalactic medium and absorption lines.

(2) To provide an interactive learning experience. The best way to learn is to make it an enjoyable experience from the start. We do not however want people to take part necessarily because they want to learn about these topics. Being entertained is enough, and familiarity with these topics will come about through the way the game is designed.

(3) To reach the largest audience possible. Given that only small fraction of the target audience is familiar with the above concepts we take the view that there is a huge amount to be gained from disseminating even simplified knowledge among a number of people which is enormous compared to the usual outreach channels (lectures etc..). The gains of this broader impact would be to increase interest in science as a career across a desirable demographic.

## 6.1 Minecraft Astronomy lesson plans

We propose to make lesson plans for elementary and middle school students to learn the size scales of the Universe and understand the elemental content of the Universe using the popular game Minecraft. Minecraft is akin to digital Lego bricks players inhabit a three-dimensional world of blocks with its own unique ecosystem and physical laws. Using imagination, players build whatever they can dream up by mining resources, combining, and placing them to build everything from pickaxes to complex and working electrical systems. So far, 100 million people have purchased the Mac/PC version of the game. It is considered a sandbox game, providing nearly limitless opportunities to build. Teachers can buy discounted licenses through MinecraftEdu.com, as well as a plug-in to tailor the software to a specific curriculum.

As an educational tool, Minecraft teaches design, collaboration, co-creating and problem solving. Its an active learning environment. Previously, successful physics lessons have been created for studying quantum mechanics (q-Craft Curriculum Project) and testing gravity (Rhett Alain, Wired) in Minecraft. Gamers enjoy making maps, building things and solving puzzles. Our Minecraft Astronomy elementary school tutorial will give instructions on how to build a rocket and how to use it to navigate a map of the Universe hosted on our server. Our middle school tutorial will include plans to build a telescope and how to use it to find the atoms that make up our Universe. Self-driven inquiry leads to locations on our maps where the content is kept up-to-date. Blog posts will connect users, guide them in reflective, big picture thought processes, craft intuitive thinking and inspire their natural curiosity. Astronomy facts, paired with math, cosmic pictures and stories will enrich learning.

One lesson plan will be primarily for 1st to 4th graders and will focus on the size scale of the solar system. We have substantial experience in this topic as the PI has been carrying outreach to this demographic since 2002, as part of the CMU Physics department's outreach program. Some of the outreach activities involved

making scale models of the solar system with household objects. Several limitations can be overcome by using the Minecraft world to do this, including extending the scale of the models arbitrarily, and using the 3rd dimension. A second lesson plan will focus on the atomic content of the Universe for middle school students (5th to 7th grade). Game users will hunt to find the rare metals among the hydrogen and helium atoms of the universe, finding the prized heavy elements in places like rocky bodies and supernovae remnants. We will develop worlds based on several different length scales, including one where we will import galaxy redshift survey data (from the SDSS) so that the students can fly around and explore the large scale structure of the Universe. It is simple to import such data sets and edit them- an example of biological molecules taken from the Molcraft project (University of Hull, UK) is shown in Figure 8 and it is easy to imagine how astronomical data would work in this environment.

Overworld dimensions of the square game plane are  $3.59 \times 10^9$  square kilometers (as compared to the Earth's spherical  $5.09 \times 10^8$  square kilometer area). The height is 256 blocks, but a Sky Dimension of similar size to the Overworld is planned for a future release. A shared world will be created and gamer guides released to aid exploration. For teachers, lesson plans will be made, including objectives and goals based on educational standards, a prior knowledge test, directed instruction, vocabulary definitions, guided practice sets and an assessment worksheet. As our work progresses, we plan to bring these lessons to a local school for tests with students. These include such schools as Colfax School, Milliones School and Helen Faison academy which we have worked with before, and where there are high fractions of students from minorities underrepresented in science. While these lessons will be available to the general public, they will be geared toward educators to be used in classrooms.

## 6.2 Universe Sandbox Tutorial

For high school students, we propose using the commercial software Universe Sandbox2 (universesandbox.com) to build a Lyman-alpha forest tutorial and activity. Universe Sandbox is an interactive space simulator, giving players the ability to wander through sections of the known universe. Universe Sandbox2 is a fully featured, space simulator, with new features and simulations added based on community requests. Players have the ability to observe and change the universe by altering fundamental constants (like the strength of gravity) and by moving celestial objects through space and time. Our high school and introductory college astronomy lesson will walk students through a Lyman-alpha forest simulation to show intervening material at differing redshifts. The material creates a forest of absorption lines and the tutorial will explain how that is seen in the visual in quasar spectra, using diagrams and an interactive applet that allows the students to change the density, distance, ionization level and elemental content of the intervening material. The user's discovery process will be framed as a quest to explain the mystery of changes in the quasar spectrum, as told in comic storyboard form following the initial discoveries of Martin Schmidt and Cyril Hazard.

Lectures, books, and video are all linear, and linear media are poor at conveying complex systems. The best way to understand a complex system is to play with it, getting a holistic sense of how parts are connected. Such systems that are best learned through simulations include the human circulatory system and nuclear reactors. In physics, demonstrations and laboratories are all simulations, traditionally with physical objects, apparatus, and measuring devices. The Universe itself is the ultimate complex physical system and arguably the most exciting one to approach in this way.

## 7 Project management and timeline

The projects will be carried out by two graduate students (one supported jointly by the grant and a TA position), the two PI/Co-PI faculty members, outreach coordinator Turnshek, and undergraduate researchers.

**Year 1.** In the first year, the initial mock datasets will be generated, both sources and lenses. The PI and a graduate student will coordinate and will be responsible for the forest lensing sources, the Co-PI and other graduate student will work on the galaxy source field. Both graduate students and undergraduates will combine these with the lens fields. The PI and Co-PI and graduate students will work on estimators, and start



on first detections from CLAMATO an a subsample of DES clusters. Turnshek will write the Minecraft lesson plans, build the worlds with the UG students and test them on local schools

**Year 2:** The graduate student will lead a study of systematic selection and instrumental effects in the galaxy and forest mocks. The PI will assemble a dataset drawn from all SDSS eBOSS spectra taken up to that point, and start scaling up the estimator code to handle millions of sightlines . The Co-I, graduate student and undergraduates will investigate the predictions for clustering statistics from the mocks and the potential for cosmological constraints. Turnshek will initiate the Universe Sandbox lesson plans.

**Year 3:** The PI and graduate student will make precise measurements of the matter power spectrum from Ly $\alpha$  lensing in the eBOSS data. The Co-I will make determinations of cluster masses from the up-to-date DES data. Both PI and Co-I and students will evaluate cosmological constraints. Turnshek will evaluate the success of the lesson plans and prepare them for wider distribution.

## 8 Results from prior NSF support

PI Croft is the PI of NSF award AST-1412966 (\$593K, 07/14-06/18 including no-cost extension), titled “Gravitational redshifts of galaxy clusters and large-scale structure: New probes of modified gravity and dark matter”. The project seeks to transform the study of gravitational redshifts and their associated redshift distortions into a major branch of cosmology. *Intellectual merit:* The results of the project so far are (1) making theoretical predictions for modified gravity and dark matter models and the effects of other asymmetric redshift distortions. (2) Formulating optimal statistical estimators to measure gravitational redshifts in galaxy clusters and from large-scale structure. (3) Making the first detection of pairwise gravitational redshifts from large-scale structure. (4) Making competitive constraints on deviations from General Relativity by combining the observational measurements and comparing to model predictions. These have been published as seven articles so far (Alam et al., 2015; Zhu et al., 2017a; Alam et al., 2017a,c; Giusarma et al., 2017; Alam et al., 2017b, 2016). *Broader Impacts:* Apart from a total of 7 outreach presentations to Middle School students, the White House Frontiers Conference and the Allegheny observatory carried out so far, the main broad impact of the project is through the dissemination of a Cosmology video game. Six undergraduate students have worked on this part of the project so far.

Co-I Scott Dodelson was co-I of NSF PHY-1125897: “Physics Frontier Center at KICP”, and Award of \$22M spanning 2011–2017. *Intellectual merit* While supported by the Physics Frontier Center proposal, Dodelson wrote 72 papers. Three of them are particularly relevant to this proposal. First, he and student Eric Baxter led the effort to detect CMB lensing around galaxy clusters using data from the South Pole Telescope Baxter et al. (2015). This 3-sigma detection set the stage for CMB cluster lensing emerging as one of the key elements in the proposal for CMB-S4 and more recently to yet another detection Baxter et al. (2017), this one using clusters found by the Dark Energy Survey (DES). A second important thrust was to carry out one of the first *de-lensing* studies of CMB polarization Manzotti et al. (2017). Finally, Dodelson recently led the analysis that combined probes in the Dark Energy Survey (DES) to produce the most constraining results yet from cosmic structure Abbott et al. (2017). This effort is one of the first of a new breed of cosmological analyses, where multiple probes are combined; we expect the same sort of synergy between the new probe proposed here and other existing probes. *Broader impacts* Dodelson was involved in the KICP outreach activities over the lifetime of the grant, which involved Cosmology Short Courses - pioneering professional development for museum and planetarium staff designed to help bring current research into the museum and classroom. Museum Partnerships - collaborations with museums to create exhibits, shows, and programming that share cosmological research with broad and diverse audiences. Space Explorers - multifaceted, multi-year commitments to inner city, minority, precollege students that included laboratory experiences, and residential science institutes at Yerkes Observatory

# REFERENCES

- Abbott, T. M. C. et al., 2017, *Dark Energy Survey Year 1 Results: Cosmological Constraints from Galaxy Clustering and Weak Lensing*.
- Alam, S., Croft, R. A. C., Ho, S., Zhu, H., and Giusarma, E., 2017a, *Relativistic effects on galaxy redshift samples due to target selection*, *Mon. Not. R. astr. Soc.*, 471, 2077–2087.
- Alam, S., Ho, S., and Silvestri, A., 2016, *Testing deviations from  $\Lambda$ CDM with growth rate measurements from six large-scale structure surveys at  $z = 0.06$ –1*, *Mon. Not. R. astr. Soc.*, 456, 3743–3756.
- Alam, S., Ho, S., Vargas-Magaña, M., and Schneider, D. P., 2015, *Testing general relativity with growth rate measurement from Sloan Digital Sky Survey - III. Baryon Oscillations Spectroscopic Survey galaxies*, *Mon. Not. R. astr. Soc.*, 453, 1754–1767.
- Alam, S., Miyatake, H., More, S., Ho, S., and Mandelbaum, R., 2017b, *Testing gravity on large scales by combining weak lensing with galaxy clustering using CFHTLenS and BOSS CMASS*, *Mon. Not. R. astr. Soc.*, 465, 4853–4865.
- Alam, S., Zhu, H., Croft, R. A. C., Ho, S., Giusarma, E., and Schneider, D. P., 2017c, *Relativistic distortions in the large-scale clustering of SDSS-II BOSS CMASS galaxies*, *Mon. Not. R. astr. Soc.*, 470, 2822–2833.
- Baxter, E. J., Rozo, E., Jain, B., Rykoff, E., and Wechsler, R. H., 2016, *Constraining the mass-richness relationship of redMaPPer clusters with angular clustering*, *Mon. Not. R. astr. Soc.*, 463, 205–221.
- Baxter, E. J. et al., 2015, *A Measurement of Gravitational Lensing of the Cosmic Microwave Background by Galaxy Clusters Using Data from the South Pole Telescope*, *Astrophys. J.*, 806 (2), 247.
- , 2017, *A Measurement of CMB Cluster Lensing with SPT and DES Year 1 Data*.
- Bi, H., 1993, *Lyman-alpha absorption spectrum of the primordial intergalactic medium*, *Ap. J.*, 405, 479–490.
- Bi, H. and Davidsen, A. F., 1997, *Evolution of Structure in the Intergalactic Medium and the Nature of the Ly $\alpha$  Forest*, *Ap. J.*, 479, 523–542.
- Blandford, R. D. and Narayan, R., 1992, *Cosmological applications of gravitational lensing*, *ARA&A*, 30, 311–358.
- Böhm, V., Schmittfull, M., and Sherwin, B. D., 2016, *Bias to CMB lensing measurements from the bispectrum of large-scale structure*, *Phys. Rev. D*, 94 (4), 043519.
- Böhm, V., Sherwin, B. D., Liu, J., Hill, J. C., Schmittfull, M., and Namikawa, T., 2018, *On the effect of non-Gaussian lensing deflections on CMB lensing measurements*, ArXiv e-prints.
- Bolton, J. S., Puchwein, E., Sijacki, D., Haehnelt, M. G., Kim, T.-S., Meiksin, A., Regan, J. A., and Viel, M., 2017, *The Sherwood simulation suite: overview and data comparisons with the Lyman  $\alpha$  forest at redshifts 2 to 5*, *Mon. Not. R. astr. Soc.*, 464, 897–914.
- Busca, N. G., Delubac, T., Rich, J., Bailey, S., Font-Ribera, A., Kirkby, D., Le Goff, J.-M., Pieri, M. M., Slosar, A., Aubourg, É., and Bautista, J. E. title = "Baryon acoustic oscillations in the Ly $\alpha$  forest of BOSS quasars", *J. A&A. a. . a. e. . . p. . a.-p. k. . c. y. . m. . a. v. . . e. . A. p. . A. d. . . a. . h. a. . P.*
- Cen, R., Miralda-Escudé, J., Ostriker, J. P., and Rauch, M., 1994, *Gravitational collapse of small-scale structure as the origin of the Lyman-alpha forest*, *Ap. J. Lett.*, 437, L9–L12.
- Cisewski, J., Croft, R. A. C., Freeman, P. E., Genovese, C. R., Khandai, N., Ozbek, M., and Wasserman, L., 2014, *Non-parametric 3D map of the intergalactic medium using the Lyman-alpha forest*, *Mon. Not. R. astr. Soc.*, 440, 2599–2609.
- Croft, R. A. C., 2004, *Ionizing Radiation Fluctuations and Large-Scale Structure in the Ly $\alpha$  Forest*, *Ap. J.*, 610, 642–662.
- Croft, R. A. C., Hu, W., and Davé, R., 1999, *Cosmological Limits on the Neutrino Mass from the Ly $\alpha$  Forest*, *Physical Review Letters*, 83, 1092–1095.
- Croft, R. A. C., Romeo, A., and Metcalf, R. B., 2018, *Weak lensing of the Lyman  $\alpha$  forest*, *Mon. Not. R. astr. Soc.*, 477, 1814–1821.
- Dark Energy Survey Collaboration, Abbott, T., Abdalla, F. B., Aleksić, J., Allam, S., Amara, A., Bacon, D., Balbinot, E., Banerji, M., Bechtol, K., Benoit-Lévy, A., Bernstein, G. M., Bertin, E., Blazek, J., Bonnett, C., Bridle, S., Brooks, D., Brunner, R. J., Buckley-Geer, E., Burke, D. L., Caminha, G. B., Capozzi, D., Carlsen, J., Carnero-Rosell, A., Carollo, M., Carrasco-Kind, M., Carretero, J., Castander, F. J., Clerkin,

- L., Collett, T., Conselice, C., Crocce, M., Cunha, C. E., D’Andrea, C. B., da Costa, L. N., Davis, T. M., Desai, S., Diehl, H. T., Dietrich, J. P., Dodelson, S., Doel, P., Drlica-Wagner, A., Estrada, J., Etherington, J., Evrard, A. E., Fabbri, J., Finley, D. A., Flaughner, B., Foley, R. J., Fosalba, P., Frieman, J., García-Bellido, J., Gaztanaga, E., Gerdes, D. W., Giannantonio, T., Goldstein, D. A., Gruen, D., Gruendl, R. A., Guarnieri, P., Gutierrez, G., Hartley, W., Honscheid, K., Jain, B., James, D. J., Jeltama, T., Jouvel, S., Kessler, R., King, A., Kirk, D., Kron, R., Kuehn, K., Kuropatkin, N., Lahav, O., Li, T. S., Lima, M., Lin, H., Maia, M. A. G., Makler, M., Manera, M., Maraston, C., Marshall, J. L., Martini, P., McMahon, R. G., Melchior, P., Merson, A., Miller, C. J., Miquel, R., Mohr, J. J., Morice-Atkinson, X., Naidoo, K., Neilsen, E., Nichol, R. C., Nord, B., Ogando, R., Ostrovski, F., Palmese, A., Papadopoulos, A., Peiris, H. V., Peoples, J., Percival, W. J., Plazas, A. A., Reed, S. L., Refregier, A., Romer, A. K., Roodman, A., Ross, A., Roza, E., Rykoff, E. S., Sadeh, I., Sako, M., Sánchez, C., Sanchez, E., Santiago, B., Scarpine, V., Schubnell, M., Sevilla-Noarbe, I., Sheldon, E., Smith, M., Smith, R. C., Soares-Santos, M., Sobreira, F., Soumagnac, M., Suchyta, E., Sullivan, M., Swanson, M., Tarle, G., Thaler, J., Thomas, D., Thomas, R. C., Tucker, D., Vieira, J. D., Vikram, V., Walker, A. R., Wechsler, R. H., Weller, J., Wester, W., Whiteway, L., Wilcox, H., Yanny, B., Zhang, Y., and Zuntz, J., 2016, *The Dark Energy Survey: more than dark energy - an overview*, *Mon. Not. R. astr. Soc.*, 460, 1270–1299.
- Elvin-Poole, J. et al., 2018, *Dark Energy Survey year 1 results: Galaxy clustering for combined probes*, *Phys. Rev.*, D98 (4), 042006.
- Giocoli, C., Jullo, E., Metcalf, R. B., de la Torre, S., Yepes, G., Prada, F., Comparat, J., Göttlober, S., Kyplin, A., Kneib, J.-P., Petkova, M., Shan, H. Y., and Tessore, N., 2016, *Multi Dark Lens Simulations: weak lensing light-cones and data base presentation*, *Mon. Not. R. astr. Soc.*, 461, 209–223.
- Giusarma, E., Alam, S., Zhu, H., Croft, R. A. C., and Ho, S., 2017, *Relativistic asymmetries in the galaxy cross-correlation function*, ArXiv e-prints.
- Hearin, A. P., Zentner, A. R., Ma, Z., and Huterer, D., 2010, *A General Study of the Influence of Catastrophic Photometric Redshift Errors on Cosmology with Cosmic Shear Tomography*, *Ap. J.*, 720, 1351–1369.
- Hernquist, L., Katz, N., Weinberg, D. H., and Miralda-Escudé, J., 1996, *The Lyman-Alpha Forest in the Cold Dark Matter Model*, *Ap. J. Lett.*, 457, L51.
- Hoekstra, H. and Jain, B., 2008, *Weak Gravitational Lensing and Its Cosmological Applications*, *Annual Review of Nuclear and Particle Science*, 58, 99–123.
- Hu, W., 2001, *Mapping the dark matter through the cmb damping tail*, *Astrophys. J.*, 557, L79–L83.
- Hu, W. and Okamoto, T., 2002, *Mass Reconstruction with Cosmic Microwave Background Polarization*, *Ap. J.*, 574, 566–574.
- Keating, L. C., Puchwein, E., and Haehnelt, M. G., 2017, *Spatial fluctuations of the intergalactic temperature-density relation after hydrogen reionization*, ArXiv e-prints.
- Kilbinger, M., 2015, *Cosmology with cosmic shear observations: a review*, *Reports on Progress in Physics*, 78 (8), 086901.
- Landy, S. D. and Szalay, A. S., 1993, *Bias and variance of angular correlation functions*, *Ap. J.*, 412, 64–71.
- Le Goff, J. M., Magneville, C., Rollinde, E., Peirani, S., Petitjean, P., Pichon, C., Rich, J., Yeche, C., Aubourg, E., Busca, N., Charlassier, R., Delubac, T., Hamilton, J. C., Palanque Delabrouille, N., Pâris, I., and Vargas Magaña, M., 2011, *Simulations of BAO reconstruction with a quasar Ly- $\alpha$  survey*, *A&A*, 534, A135.
- Lee, K.-G., Bailey, S., Bartsch, L. E., Carithers, W., Dawson, K. S., Kirkby, D., Lundgren, B., Margala, D., Palanque-Delabrouille, N., Pieri, M. M., Schlegel, D. J., Weinberg, D. H., Yèche, C., Aubourg, É., Bautista, J., Bizyaev, D., Blomqvist, M., Bolton, A. S., Borde, A., Brewington, H., Busca, N. G., Croft, R. A. C., Delubac, T., Ebelke, G., Eisenstein, D. J., Font-Ribera, A., Ge, J., Hamilton, J.-C., Hennawi, J. F., Ho, S., Honscheid, K., Le Goff, J.-M., Malanushenko, E., Malanushenko, V., Miralda-Escudé, J., Myers, A. D., Noterdaeme, P., Oravetz, D., Pan, K., Pâris, I., Petitjean, P., Rich, J., Rollinde, E., Ross, N. P., Rossi, G., Schneider, D. P., Simmons, A., Snedden, S., Slosar, A., Spergel, D. N., Suzuki, N., Viel, M., and Weaver, B. A., 2013, *The BOSS Ly $\alpha$  Forest Sample from SDSS Data Release 9*, *Astron. J.*, 145, 69.
- Lee, K.-G., Hennawi, J. F., Stark, C., Prochaska, J. X., White, M., Schlegel, D. J., Eilers, A.-C., Arinyo-

- i-Prats, A., Suzuki, N., Croft, R. A. C., Caputi, K. I., Cassata, P., Ilbert, O., Garilli, B., Koekemoer, A. M., Le Brun, V., Le Fèvre, O., Maccagni, D., Nugent, P., Taniguchi, Y., Tasca, L. A. M., Tresse, L., Zamorani, G., and Zucca, E., 2014, *Ly $\alpha$  Forest Tomography from Background Galaxies: The First Megaparsec-resolution Large-scale Structure Map at  $z$  greater than 2*, *Ap. J. Lett.* , 795, L12.
- Lee, K.-G., Krolewski, A., White, M., Schlegel, D., Nugent, P. E., Hennawi, J. F., Müller, T., Pan, R., Prochaska, J. X., Font-Ribera, A., Suzuki, N., Glazebrook, K., Kacprzak, G. G., Kartaltepe, J. S., Koekemoer, A. M., Le Fèvre, O., Lemaux, B. C., Maier, C., Nanayakkara, T., Rich, R. M., Sanders, D. B., Salvato, M., Tasca, L., and Tran, K.-V. H., 2018, *First Data Release of the COSMOS Ly $\alpha$  Mapping and Tomography Observations: 3D Ly $\alpha$  Forest Tomography at  $2.05 < z < 2.55$* , *ApJS*, 237, 31.
- Lewis, A. and Challinor, A., 2006, *Weak gravitational lensing of the CMB*, *Physics Reports*, 429, 1–65.
- Lewis, A. and Pratten, G., 2016, *Effect of lensing non-Gaussianity on the CMB power spectra*, *J. Cosmo. & Astroparticle Phys.*, 12, 003.
- Liu, J. et al., 2015, *Analysis of Sunyaev-Zel’dovich effect massobservable relations using South Pole Telescope observations of an X-ray selected sample of low-mass galaxy clusters and groups*, *Mon. Not. Roy. Astron. Soc.*, 448 (3), 2085–2099.
- Loveide, M., Marnerides, S., Hui, L., Ménard, B., and Lidz, A., 2010, *Gravitational lensing as signal and noise in Lyman- $\alpha$  forest measurements*, *Phys. Rev. D* , 82 (10), 103507.
- Manzotti, A. et al., 2017, *CMB Polarization B-mode Delensing with SPTpol and Herschel*, *Astrophys. J.*, 846 (1), 45.
- Melchior, P., Gruen, D., McClintock, T., Varga, T. N., Sheldon, E., Rozo, E., Amara, A., Becker, M. R., Benson, B. A., Bermeo, A., Bridle, S. L., Clampitt, J., Dietrich, J. P., Hartley, W. G., Hollowood, D., Jain, B., Jarvis, M., Jeltama, T., Kacprzak, T., MacCrann, N., Rykoff, E. S., Saro, A., Suchyta, E., Troxel, M. A., Zuntz, J., Bonnett, C., Plazas, A. A., Abbott, T. M. C., Abdalla, F. B., Annis, J., Benoit-Lévy, A., Bernstein, G. M., Bertin, E., Brooks, D., Buckley-Geer, E., Carnero Rosell, A., Carrasco Kind, M., Carretero, J., Cunha, C. E., D’Andrea, C. B., da Costa, L. N., Desai, S., Eifler, T. F., Flaugher, B., Fosalba, P., García-Bellido, J., Gaztanaga, E., Gerdes, D. W., Gruendl, R. A., Gschwend, J., Gutierrez, G., Honscheid, K., James, D. J., Kirk, D., Krause, E., Kuehn, K., Kuropatkin, N., Lahav, O., Lima, M., Maia, M. A. G., March, M., Martini, P., Menanteau, F., Miller, C. J., Miquel, R., Mohr, J. J., Nichol, R. C., Ogando, R., Romer, A. K., Sanchez, E., Scarpine, V., Sevilla-Noarbe, I., Smith, R. C., Soares-Santos, M., Sobreira, F., Swanson, M. E. C., Tarle, G., Thomas, D., Walker, A. R., Weller, J., and Zhang, Y., 2017, *Weak-lensing mass calibration of redMaPPer galaxy clusters in Dark Energy Survey Science Verification data*, *Mon. Not. R. astr. Soc.*, 469, 4899–4920.
- Metcalf, R. B., Croft, R. A. C., and Romeo, A., 2017, *Noise Estimates for Measurements of Weak Lensing from the Lyman-alpha Forest*, *ArXiv e-prints*.
- , 2018, *Noise estimates for measurements of weak lensing from the Ly  $\alpha$  forest*, *Mon. Not. R. astr. Soc.*, 477, 2841–2847.
- Metcalf, R. B. and Petkova, M., 2014, *GLAMER - I. A code for gravitational lensing simulations with adaptive mesh refinement*, *Mon. Not. R. astr. Soc.*, 445, 1942–1953.
- Palanque-Delabrouille, N., Yèche, C., Baur, J. and Magneville, C., Rossi, G., Lesgourgues, J., Borde, A., Burtin, E., LeGoff, J.-M., Rich, J., Viel, M., and Weinberg, D., 2015, *Neutrino masses and cosmology with Lyman-alpha forest power spectrum*, *JCAP*, 11, 011.
- Peebles, M. S., Weinberg, D. H., Davé, R., Fardal, M. A., and Katz, N., 2010, *Pressure support versus thermal broadening in the Lyman  $\alpha$  forest - I. Effects of the equation of state on longitudinal structure*, *Mon. Not. R. astr. Soc.*, 404, 1281–1294.
- Peirani, S., Weinberg, D. H., Colombi, S., Blaizot, J., Dubois, Y., and Pichon, C., 2014, *LyMAS: Predicting Large-scale Ly $\alpha$  Forest Statistics from the Dark Matter Density Field*, *Ap. J.* , 784, 11.
- Petkova, M., Metcalf, R. B., and Giocoli, C., 2014, *GLAMER - II. Multiple-plane gravitational lensing*, *Mon. Not. R. astr. Soc.*, 445, 1954–1966.
- Rauch, M., 1998, *The Lyman Alpha Forest in the Spectra of QSOs*, *ARA&A*, 36, 267–316.
- Savaglio, S., Panagia, N., and Padovani, P., 2002, *The Ly $\alpha$  Forest of a Lyman Break Galaxy: Very Large*

- Telescope Spectra of MS 1512-cB58 at  $z=2.724$* , *Ap. J.* , 567, 702–711.
- Scranton, R., Ménard, B., Richards, G. T., Nichol, R. C., Myers, A. D., Jain, B., Gray, A., Bartelmann, M., Brunner, R. J., Connolly, A. J., Gunn, J. E., Sheth, R. K., Bahcall, N. A., Brinkman, J., Loveday, J., Schneider, D. P., Thakar, A., and York, D. G., 2005, *Detection of Cosmic Magnification with the Sloan Digital Sky Survey*, *Ap. J.* , 633, 589–602.
- Simet, M., McClintock, T., Mandelbaum, R., Rozo, E., Rykoff, E., Sheldon, E., and Wechsler, R. H., 2017, *Weak lensing measurement of the mass-richness relation of SDSS redMaPPer clusters*, *Mon. Not. R. astr. Soc.*, 466, 3103–3118.
- Walsh, D., Carswell, R. F., and Weymann, R. J., 1979, *0957 + 561 A, B - Twin quasistellar objects or gravitational lens*, *Nature*, 279, 381–384.
- Zentner, A. R., Semboloni, E., Dodelson, S., Eifler, T., Krause, E., and Hearin, A. P., 2013, *Accounting for baryons in cosmological constraints from cosmic shear*, *Phys. Rev. D* , 87 (4), 043509.
- Zhang, Y., Anninos, P., and Norman, M. L., 1995, *A Multispecies Model for Hydrogen and Helium Absorbers in Lyman-Alpha Forest Clouds*, *Ap. J. Lett.* , 453, L57.
- Zhu, H., Alam, S., Croft, R. A. C., Ho, S., and Giusarma, E., 2017a, *N-body simulations of gravitational redshifts and other relativistic distortions of galaxy clustering*, *Mon. Not. R. astr. Soc.*, 471, 2345–2356.
- , 2017b, *N-body simulations of gravitational redshifts and other relativistic distortions of galaxy clustering*, *Mon. Not. R. astr. Soc.*, 471, 2345–2356.
- Zu, Y., Weinberg, D. H., Rozo, E., Sheldon, E. S., Tinker, J. L., and Becker, M. R., 2014, *Cosmological constraints from the large-scale weak lensing of SDSS MaxBCG clusters*, *Mon. Not. R. astr. Soc.*, 439, 1628–1647.